



^{13}C - ^{14}C relations reveal that soil ^{13}C -depth gradient is linked to historical changes in vegetation ^{13}C

Alexia Paul · Jérôme Balesdent · Christine Hatté

Received: 1 July 2019 / Accepted: 22 November 2019 / Published online: 6 December 2019
© Springer Nature Switzerland AG 2019

Abstract

Aims The understanding of the dynamics of subsoil (>30 cm) soil organic matter (SOM) is critical to predict the future evolution of the carbon cycle. Stable carbon isotopes ratios ($^{13}\text{C}/^{12}\text{C}$) are helpful to study the dynamics of SOM, but their variations with depth are still speculative.

Methods Several studies indicated that the $^{13}\text{C}/^{12}\text{C}$ ratio of C_3 vegetation decreased over time more than that of atmospheric CO_2 did. From these studies, we modelled the average variation of $\delta^{13}\text{C}$ values of vegetation from 20,000 years Before Present (BP) to today. Then, we conducted a meta-analysis of the $\delta^{13}\text{C}$ vs $\Delta^{14}\text{C}$ values relations in forty-five soil profiles sampled all around the world.

Results We first found evidence of the change in SOM $\delta^{13}\text{C}$ values with the sampling year of the profile. Then, by converting $\Delta^{14}\text{C}$ values into mean calendar age of SOM, we showed that 40% of the change in SOM $\delta^{13}\text{C}$ values was explained by the historical change in plant $\delta^{13}\text{C}$ values.

Conclusion We conclude that the average increase of SOM $\delta^{13}\text{C}$ values with depth was mostly linked to the change in vegetation $\delta^{13}\text{C}$ values over the last 20,000 years. The variance around the trend was attributed to the contribution of root derived carbon and to soil processes such as interaction of SOM with minerals or to microbial processes.

Keywords Soil organic carbon · Stable isotope · ^{13}C enrichment · Radiocarbon · Dating · Soil depth profile

Responsible Editor: Xinhua He.

Electronic supplementary material The online version of this article (<https://doi.org/10.1007/s11104-019-04384-4>) contains supplementary material, which is available to authorized users.

A. Paul · J. Balesdent (✉)
Aix-Marseille University, CNRS, IRD, INRA, Coll. France,
CEREGE, 13545 Aix-en-Provence, France
e-mail: jerome.balesdent@inra.fr

A. Paul (✉)
Department of Renewables Resources, University of Alberta, 442
Earth Sciences Building, Edmonton, AB T6G2E3, Canada
e-mail: alexia.choucherie@gmail.com

C. Hatté
Laboratoire des Sciences du Climat et de l'Environnement,
LSCE/IPSL, UMR 8212 CEA-CNRS-UVSQ, Université Paris
Saclay, F-91191 Gif-sur-Yvette, France

Introduction

Carbon exchanges between soil and atmosphere are of great concern for the understanding of the global carbon cycle and therefore for the understanding of climate change. Carbon from plants in the form of organic matter can be stabilized and stored in soil for thousands of years, in particular in subsoils (below 30 cm). However, the fate of subsoil carbon is not well understood. In addition to the fact that deep soils contain twice as much carbon as surface soils (Jobbagy and Jackson 2000), the organic matter is also older, as revealed by the universal decrease in ^{14}C content with depth (Mathieu et al. 2015).

Soil carbon profiles behave as a dynamic system, which results from several processes acting together: the history of carbon inputs, the depth distribution of the latter, biodegradation processes, and various degrees of movement of dissolved or solid matter, including bioturbation that continuously buries surficial matter and brings deep soil material to the surface (Elzein and Balesdent 1995). In such systems, the organic matter contains a full age distribution from the youngest (recent plant- and root-derived products) to the very old, stabilized carbon. Statistically, the youngest organic matter has experienced fewer biodegradation cycles and is found closer to the surface.

The isotopic composition of carbon in SOM has often been used as a tool to understand organic matter dynamics through the $^{14}\text{C}/^{12}\text{C}$ and $^{13}\text{C}/^{12}\text{C}$ ratios (Campbell et al. 1967; Rafter and Stout 1970; Wang et al. 2018; Balesdent et al. 2018), where the ^{14}C signal of organic matter is an indicator of its age, and the ^{14}C content from nuclear bombs was further used to estimate the residence times of carbon in soils (Gaudinski et al. 2000; He et al. 2016), or the factors governing its stabilization (Mathieu et al. 2015). Several studies also recorded the ^{13}C isotopic composition of soil carbon in order to investigate the stabilization of organic matter at depth (Poage and Feng 2004; Wynn et al. 2005), and an increase in $\delta^{13}\text{C}$ values with depth has systematically been observed under C_3 plant, on average by 1 to 3‰ in the first meter (Balesdent et al. 1993; Brüggemann et al. 2011). The reasons for this $\delta^{13}\text{C}$ values enrichment are not yet fully known. Different mechanisms can be involved. Firstly, the absolute $\delta^{13}\text{C}$ values of vegetation may have decreased with time (Boström et al. 2007). Post-photosynthesis fractionation may also occur since root materials are ^{13}C -enriched compared to leaves (Gessler et al. 2007; Werth and Kuzyakov 2010). Secondly, true mass-dependent isotope fractionation may occur in the combined process of microbial respiration and microbial biosynthesis, so that residual products would be progressively ^{13}C -enriched during the continuous degradation process, when compared to initial plant material as reviewed by Werth and Kuzyakov (2010). Decomposition may also select ^{13}C -enriched or ^{13}C -depleted components by differential microbial use efficiency or decay rate between molecules (Boström et al. 2007). Finally, the movement of organic matter within the soil profile (e.g. in the form of dissolved organic carbon) may lead to the accumulation of ^{13}C -enriched or ^{13}C -depleted compounds downwards

(Kaiser et al. 2001). Incorporation of inorganic carbon atoms by heterotrophic microorganism (dark CO_2 fixation) may also increase SOM $^{13}\text{C}/^{12}\text{C}$ isotope ratios by adding atoms that have the isotopic composition of atmospheric CO_2 , but the extent of the process has been considered as negligible (Šantrůčková et al. 2018).

Some of these studies focused on proposing mechanisms behind the ^{13}C enrichment with depth and based their work on the assumption that vegetation in equilibrium with soil maintained constant $\delta^{13}\text{C}$ values. However, there are evidences that the vegetation $\delta^{13}\text{C}$ values has changed over time. The more recent change is due to fossil fuel burning and land use change during the last 150 years of Human activities, resulting in both an increase in pCO_2 (the partial pressure of carbon dioxide in the atmosphere) and a dilution of the ^{13}C of atmospheric CO_2 by ^{13}C depleted emitted CO_2 (i.e. “Suess effect”, Keeling et al. 1995, 1979). The depletion in atmospheric $\delta^{13}\text{CO}_2$ values leads to a more ^{13}C -depleted vegetation biomass during photosynthesis (Farquhar et al. 1989). The “Suess effect” is considered now to be part of the ^{13}C -depletion of SOM in surface soil (Boström et al. 2007; Brecker et al. 2015; Brunn et al. 2016, 2017).

In addition, elevation of pCO_2 -from ca. 190 ppm prior to 17,500 BP (Before Present i.e. before 1950) up to 408 ppm in 2018 (US Department of Commerce 2017) - is expected to affect the fractionation process due to the change in stomatal conductance regulation in plants in order to balance the carbon input and to increase the intrinsic water-use efficiency (Keeling et al. 2017). Hence, several environmental studies have shown a relation between pCO_2 and the isotope fractionation by C_3 plant photosynthesis (Krishnamurthy and Epstein 1990; Van de Water et al. 1994; Feng and Epstein 1995; Pasquier-Cardin et al. 1999; Schubert and Jahren 2015; Voelker et al. 2016; Keeling et al. 2017). All but one (Kohn 2016) have concluded that the increase in pCO_2 induces a decrease in $\delta^{13}\text{C}$ values of C_3 -plant, leading to a decrease in the $\delta^{13}\text{C}$ values of the vegetation ranging between 2.4 ‰ (Keeling et al. 2017) and 4.9 ‰ (Schubert and Jahren 2015) when CO_2 increases from 190 to 400 ppm.

Our objective is to evaluate the impact of the changes of vegetation $\delta^{13}\text{C}$ on the vertical distribution of $\delta^{13}\text{C}$ values in SOM. We have first reconstructed a global trend of the isotopic composition of the vegetation through time by using atmospheric data and relations between pCO_2 and $\delta^{13}\text{C}$ values from four studies (Feng

and Epstein 1995; Schubert and Jahren 2015; Voelker et al. 2016; Keeling et al. 2017). Then, we compiled data from 45 soil profiles around the world where $\delta^{13}\text{C}$ and $\Delta^{14}\text{C}$ values of SOM had been measured. Considering that organic matter is older in deep horizons, we hypothesized that the change in vegetation $\delta^{13}\text{C}$ values with time is responsible for the soil ^{13}C enrichment with depth. We have tested this hypothesis by comparing the global trend of vegetation $\delta^{13}\text{C}$ with SOM $\delta^{13}\text{C}$ values.

Material and methods

Definition and vocabulary

The isotopic composition of stable carbon is reported in $\delta^{13}\text{C}$ values presented as per mil (‰) compared to Vienna Pee Dee Belemnite (V-PDB) international standard. We described in Table 1 the main terms we used in the following sections.

Atmospheric CO₂ data

Atmospheric CO₂ data are needed to reconstruct the isotopic composition of vegetation. The pre-bomb $\delta^{13}\text{C}_{\text{air}}$ and $\Delta^{14}\text{C}_{\text{air}}$ values of atmospheric CO₂ were taken from Schmitt et al. (2012) and from Reimer et al. (2009) and the post-bomb from Francey et al. (1999) and Hua et al. (2013), respectively. The pCO₂ values came from Francey et al. (1999), Schmitt et al. (2012) and from NOAA data (US Department of Commerce 2017) for the most recent dates. We performed linear interpolation when data were missing.

Vegetation $\delta^{13}\text{C}$ values

The temporal change of isotopic composition of the vegetation was reconstructed from four studies by

Table 1 Definition of the specific terms used in the text

Terms	Units	Definition
$\delta^{13}\text{C}_{\text{air}}$	‰	$\delta^{13}\text{C}$ values of the atmospheric CO ₂
$\Delta^{14}\text{C}_{\text{air}}$	‰	$\Delta^{14}\text{C}$ values of the atmospheric CO ₂
$\delta^{13}\text{C}_{\text{SOM}}$	‰	$\delta^{13}\text{C}$ values of SOM
$\Delta^{14}\text{C}_{\text{SOM}}$	‰	$\Delta^{14}\text{C}$ values of SOM
$\delta^{13}\text{C}_{\text{plant}}$	‰	$\delta^{13}\text{C}$ values of vegetation
$\delta^{13}\text{C}_{\text{sim}}$	‰	Simulation of $\delta^{13}\text{C}_{\text{SOM}}$ by taking into account the mean value of $\delta^{13}\text{C}_{\text{plant}}$
$\Delta^{13}\text{C}_{\text{SOM}}$	‰	$\delta^{13}\text{C}_{\text{SOM}} - \delta^{13}\text{C}_{\text{SOM}(\Delta^{14}\text{C}=0)}$ ^a
$\Delta^{13}\text{C}_{\text{sim}}$	‰	$\delta^{13}\text{C}_{\text{sim}} - \delta^{13}\text{C}_{\text{sim}(\Delta^{14}\text{C}=0)}$ ^a
$\Delta^{13}\text{C}_{\text{plant}}$	‰	$\delta^{13}\text{C}_{\text{plant}} - \delta^{13}\text{C}_{\text{plant}(\Delta^{14}\text{C}=0)}$ ^a

^a $\delta^{13}\text{C}_{(\Delta^{14}\text{C}=0)}$ corresponds to $\delta^{13}\text{C}$ values of SOM, sim or plant in 1950 (0 BP) based on each profile calculation by linear regression

Schubert and Jahren (2015), Feng and Epstein (1995), Voelker et al. (2016) and Keeling et al. (2017) that found a relation of the $\delta^{13}\text{C}$ values of the vegetation ($\delta^{13}\text{C}_{\text{plant}}$) with the atmospheric pCO₂. They derived their relation from the Farquhar’s equation (Farquhar et al. 1989):

$$\delta^{13}\text{C}_{\text{plant}} = \frac{\delta^{13}\text{C}_{\text{air}} - 0.0044 + \left(0.0017 * \frac{C_i}{p\text{CO}_2}\right)}{0.0044 - \left(0.0017 * \frac{C_i}{p\text{CO}_2}\right) + 1} \quad (1)$$

where C_i corresponds to the leaf intercellular space CO₂ concentration and pCO₂ to the atmospheric CO₂ concentration (ppm).

The four equations we used from the different studies are summarized below:

- From Schubert and Jahren (2015):

$$\delta^{13}\text{C}_{\text{plant}} = \frac{\delta^{13}\text{C}_{\text{air}} - (28.26 * 0.22 * (p\text{CO}_2 + 23.9)) / \left[(28.26 + (0.22 * p\text{CO}_2 + 23.9)) \right]}{(28.26 * 0.22 * (p\text{CO}_2 + 23.9)) / \left[(28.26 + (0.22 * p\text{CO}_2 + 23.9)) \right] + 1} \quad (2)$$

- From Feng and Epstein (1995), we used the linear relation between pCO_2 and $\delta^{13}C$:

$$\delta^{13}C_{plant} = \delta^{13}C_{air} - (constant - 0.02 * pCO_2) \quad (3)$$

- From Voelker et al. (2016), we calculated the term $C_i/pCO_2 = a + b * \exp.(-0.0076 * pCO_2)$; ($r^2 = 0.43$, $p < 0.05$) that we used in the Farquhar's equation (Eq. 1)
- From Keeling et al. (2017), we used the linear relation between pCO_2 and $\delta^{13}C$:

$$\delta^{13}C_{plant} = \delta^{13}C_{air} - (constant - 0.014 * pCO_2) \quad (4)$$

Taking the absolute $\delta^{13}C_{plant}$ values does not make sense because of spatial and interspecies variations, thereby we calculated for each model the difference: $\Delta^{13}C_{plant} = \delta^{13}C_{plant} - \delta^{13}C_{plant} (\Delta^{14}C = 0)$.

From Eqs. 1, 2, 3 and 4 we reconstructed a global trend of the average variations of $\Delta^{13}C_{plant}$ values over time. The current state of knowledge does not allow one scenario to be chosen over another, we decided to work with the mean value of $\Delta^{13}C_{plant}$ from the four equations.

Soil database description

Forty-five soil profiles with both $\delta^{13}C_{SOM}$ and $\Delta^{14}C_{SOM}$ values measured from the surface to deep soil were extracted from the literature. These profiles were selected from the database of Mathieu et al. (2015) that also reports sampling year, location, soil type, land-use, soil layer identification, pedological properties, climatic data, carbon content, characteristic analyses and $\delta^{13}C$ and $\Delta^{14}C$ values of more than 300 soil profiles. From this database, only $\delta^{13}C$ values measurements on bulk soil organic carbon by IRMS and C_3 plant derived profiles were chosen. The 45 profiles encompass nine soil types (Luvisol, Gleysol, Podzol, Acrisol, Ferralsol, Chernozem, Andosol, Nitisol and Cambisol, IUSS Working Group WRB 2014) and three large ecosystems (grassland, forest, and arable land). Forty-four out of the 45 were sampled from 1959 to 2009 and the last one in 1900 (See Supplementary material). The location of the 45 profiles is presented in Fig. 1 as well as the mean annual temperature; mean annual precipitation and sampling year. The references from which the $\delta^{13}C$ and

$\Delta^{14}C$ values were extracted and details of the data are presented in supplementary material.

Simulation of $\delta^{13}C$ values of soil organic matter (SOM) from $\Delta^{14}C$ values and sampling year

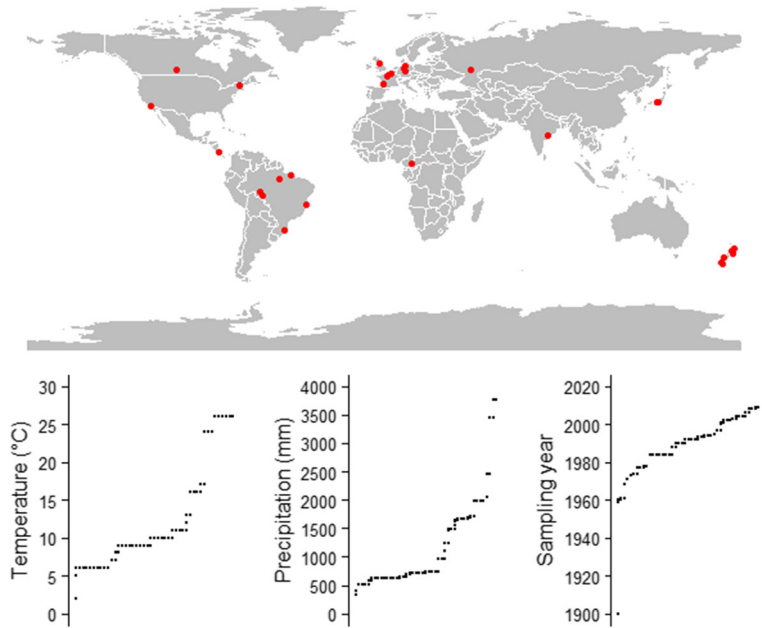
In order to compare the global change of $\delta^{13}C_{plant}$ with $\delta^{13}C_{SOM}$ values through time, we first converted $\Delta^{14}C_{SOM}$ values into age. Then, to estimate how $\delta^{13}C_{SOM}$ values were impacted by the $\delta^{13}C_{plant}$ values, we simulated changes in $\delta^{13}C_{SOM}$ values by integrating the $\delta^{13}C_{plant}$ values for each profile depending on the sampling year.

The $\Delta^{14}C$ values of SOM from the database were converted into mean calendar age according to Balesdent (1987): a mean age value α of SOM was calculated from $\Delta^{14}C_{SOM}$ values assuming an exponential distribution of ages, i.e., by solving Eq. 5:

$$\frac{\Delta^{14}C}{1000} + 1 = \frac{\int_{t=0}^{\infty} (1 + \Delta^{14}C_{air(p-t)}) * e^{-\lambda * (t+m-p)} * e^{-\frac{t}{\alpha}} * dt}{\int_{t=0}^{\infty} e^{-\frac{t}{\alpha}} * dt} \quad (5)$$

where p is the sampling year; $\Delta^{14}C_{air(p-t)}$ is the atmospheric $\Delta^{14}C$ values at the date $(p-t)$; $\Delta^{14}C_{air}$ values were obtained from atmospheric summer $\Delta^{14}C$ values records in Hua et al. (2013) and Reimer et al. (2009) taking into account the hemisphere and atmospheric zone of the studied site (Hua et al. 2013); λ is the radioactive decay constant of ^{14}C ($\ln(2)/\lambda = 5730$ years); m is the date of ^{14}C measurement and was fixed as 2 years before publication if unknown; α is the mean age of SOM at the sampling year, so that the calendar age of SOM is $p - \alpha$. Eq. (2) has two solutions for $p - \alpha$ in the cases where the $\Delta^{14}C$ values of SOM are higher than $\Delta^{14}C_{air}$ values in the sampling year, i.e., corresponding to either young post-bomb carbon or a mixture of pre-bomb and bomb-peak carbon. In that case, the younger solution was chosen for litter layers, whereas the older one was chosen for organo-mineral horizons. A few litter samples with very high $\Delta^{14}C$ values had no solution for $p - \alpha$; in that case, the calendar age was set at $\Delta^{14}C_{air(p-\infty)}$. Secondly, for each site we integrated the vegetation $\delta^{13}C_{plant}$ values as a function of carbon mean age $p - \alpha$ and sampling year using the same exponential distribution of ages. Equation (6) is similar to Eq. (5) but with no radioactive decay.

Fig. 1 Geographic distribution, range of values of mean annual temperature, mean annual precipitation, and sampling year of the 45 selected soil profiles



$$\delta^{13}C_{sim} = \frac{1}{\alpha} \int_{t=0}^{\infty} (\delta^{13}C_{plant(p-t)}) * e^{-\frac{t}{\alpha}} * dt \quad (6)$$

with $\delta^{13}C_{sim}$, the SOM $\delta^{13}C$ simulated by taking into account the mean value of $\delta^{13}C_{plant}$ calculated with Eqs. 1, 2, 3 and 4.

Statistical analyses

To study the relation between $\delta^{13}C_{SOM}$ and $\Delta^{14}C_{SOM}$ values, we calculated for each profile the linear regression of the function (taking into account the litter values):

$$\delta^{13}C_{SOM} = s * \Delta^{14}C_{SOM} + b \quad (7)$$

with b equal to $\delta^{13}C_{(\Delta^{14}C=0)}$.

To highlight the variables that affect the slope s of the function (7), we calculated linear regression with the software R (version 3.3.2.; lm function). The explanatory variables were “sampling year”, “mean annual precipitation”, “mean annual temperature”, “aridity index” (Trabucco and Zomer 2009), “elevation” and “soil type”. Significance is chosen when $p < 0.05$. The relation of the previous variables with the $\delta^{13}C$ values at the depth 0 cm and with $\delta^{13}C$ values of the litter was also tested with a linear model. The climatic data (precipitation, temperature,

and aridity index) were taken from authors’ statements or from the geographical coordinates for the modern climate (New et al. 2002). Climatic variations during the last ten thousand years were not considered.

Results

$\Delta^{14}C$ and $\delta^{13}C$ values relation in soil organic matter

The $\delta^{13}C_{SOM}$ values increased with depth on average from $-27.3 \pm 0.3\%$ at 0 cm to $-25.4 \pm 0.8\%$ at 100 cm (Fig. 2a). The $\Delta^{14}C_{SOM}$ values decreased with depth for all the profiles, on average from $180 \pm 42\%$ to $-307 \pm 85\%$ (Supplemental material), and accordingly, mean calendar age increased with depth (Fig. 2b). There was a high variability among the profiles, especially at depths where fewer samples were measured, but similar patterns were found in each profile. The $\delta^{13}C$ values at the depth 0 cm significantly depend on the sampling year. The mean absolute $\delta^{13}C_{SOM}$ values at the first 10 cm depth decreased with time: it was $-26.9 \pm 0.9\%$ for profiles sampled between 1960 and 1973 and $-28.5 \pm 0.5\%$ between 2005 and 2010. Because of the covariation with other variables, we could not estimate a significant temporal trend in ^{13}C gradient

with depth. On the contrary there is a significant temporal trend in the relation of ^{13}C - and ^{14}C -gradients with depth. The slope s of the relation between $\delta^{13}\text{C}_{\text{SOM}}$ and $\Delta^{14}\text{C}_{\text{SOM}}$ values (Eq. 7) in a given profile varies from 0.002 ± 0.001 to -0.010 ± 0.002 . We found that the slopes significantly depend on the sampling date and accordingly to the isotopic composition of the atmosphere $\delta^{13}\text{C}_{\text{air}}$ values. The slope of the relation between $\delta^{13}\text{C}_{\text{SOM}}$ and $\Delta^{14}\text{C}_{\text{SOM}}$ values was more negative for profiles sampled more recently where $\delta^{13}\text{C}_{\text{air}}$ values were also more negative (Fig. 3). As a result of the progressive incorporation of bomb- ^{14}C , $\Delta^{14}\text{C}_{\text{SOM}}$ values tend to increase with the sampling year in the topsoil, but much less in deep horizons. The negative correlation between s and sampling date therefore means that topsoil $\delta^{13}\text{C}_{\text{SOM}}$ values decrease, when $\Delta^{14}\text{C}_{\text{SOM}}$ values increase. The slope s was not significantly related with soil types.

The $\delta^{13}\text{C}_{\text{SOM}}$ values presented also a relation with the elevation where the soils were sampled. Mean annual temperature, latitude and aridity index did neither affect $\delta^{13}\text{C}$ values of SOM, nor the slope of the relation between $\delta^{13}\text{C}_{\text{SOM}}$ and $\Delta^{14}\text{C}_{\text{SOM}}$ values.

Comparing $\delta^{13}\text{C}$ values of soil ($\delta^{13}\text{C}_{\text{SOM}}$) and $\delta^{13}\text{C}$ values of vegetation ($\delta^{13}\text{C}_{\text{plant}}$)

The mean $\Delta^{13}\text{C}_{\text{plant}}$ values decreased by $4.2 \pm 0.6\%$ between 20,000 BP and 2018 AD (Anno Domini). We found that the mean values of $\Delta^{13}\text{C}_{\text{SOM}}$ (moving average of 10 points) matched the reconstructed $\Delta^{13}\text{C}_{\text{plant}}$ values through time (Fig. 4c).

To test the hypothesis that the vertical $\delta^{13}\text{C}_{\text{SOM}}$ gradient in soil is due to the historical change in vegetation $\delta^{13}\text{C}$ values, we calculated for each sample the simulated $\delta^{13}\text{C}_{\text{SOM}}$ values ($\delta^{13}\text{C}_{\text{sim}}$) by taking the isotopic composition of the vegetation (mean value of $\delta^{13}\text{C}_{\text{plant}}$) at the calendar year of SOM (Eq. 3). The observed $\Delta^{13}\text{C}_{\text{SOM}}$ value of each sample was then compared to the predicted equivalent difference, $\Delta^{13}\text{C}_{\text{sim}}$ (Table 1). The observed $\Delta^{13}\text{C}_{\text{SOM}}$ values relative to the simulated $\Delta^{13}\text{C}_{\text{sim}}$ values are shown in Fig. 5. The simulation explains 40% of the variance. Few observed $\delta^{13}\text{C}_{\text{SOM}}$ values presented a high enrichments ($> 2.5\%$) and are older than 3000 BP (Fig. 5).

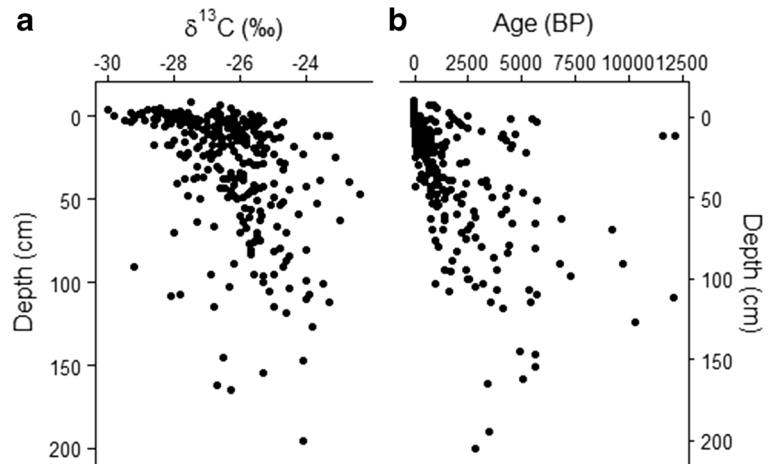
Discussion

$\delta^{13}\text{C}$ values of SOM are derived from $\delta^{13}\text{C}$ values of vegetation

The almost systematic ^{13}C -enrichment that accompanies carbon ageing with depth can be the result of temporal change in the initial composition of carbon or isotopic effects associated to soil processes. In this study, we analyzed soil ^{13}C gradients as a function of carbon age (and not depth per se), and isolated the sole effect of the change in initial $\delta^{13}\text{C}_{\text{plant}}$ values on the resulting $\delta^{13}\text{C}_{\text{SOM}}$ values. Both changes in pCO_2 and $\delta^{13}\text{C}$ values of atmospheric CO_2 induce changes in vegetation $\delta^{13}\text{C}$ values. In our panel of soil profiles, the average vertical ^{13}C gradient (Fig. 2) is similar to the expected change in vegetation $\delta^{13}\text{C}$ values (Fig. 4). Variations of $\delta^{13}\text{C}_{\text{SOM}}$ values with time (Figs. 4b, c) clearly mimic the simulated changes in $\delta^{13}\text{C}_{\text{plant}}$ values. For example, from the four studies, we calculated an average decrease in $\delta^{13}\text{C}_{\text{plant}}$ values of $2.4 \pm 0.6\%$ from 5000 BP to -50 BP (i.e. 2000 AD) and we observed an average decrease in $\delta^{13}\text{C}_{\text{SOM}}$ values of $2.5 \pm 1.5\%$ over the same period of time (Fig. 4c). Here, the values of observed $\Delta^{13}\text{C}_{\text{SOM}}$ coincide with the calculated values of $\Delta^{13}\text{C}_{\text{plant}}$ over a broad time range, i.e., both between 1000 and 3000 BP and between -30 and -50 BP (i.e. 1980 and 2000 AD, Fig. 4). The average change of $\delta^{13}\text{C}_{\text{plant}}$ values with time explains the average increase of $\delta^{13}\text{C}_{\text{SOM}}$ values with depth for the studied soil profiles. This point is supported by the relation of the gradients s with the sampling date (Fig. 3) that indicates both the impact of pCO_2 and $\delta^{13}\text{C}_{\text{atm}}$ values, with soils sampled before the 1970's having a weak gradient of $\delta^{13}\text{C}$ values. Moreover, by comparing $\Delta^{13}\text{C}_{\text{SOM}}$ values of eight soil profiles, representing the major soil types, with the mean variation of $\Delta^{13}\text{C}_{\text{plant}}$ values over time (Fig. 6), we showed that the average change in $\delta^{13}\text{C}_{\text{SOM}}$ values is attributed to the average change in $\delta^{13}\text{C}_{\text{plant}}$ values with time for very different types of soils. The mean $\delta^{13}\text{C}$ value of C_3 plants thus varied with major transitions from high values at the deglaciation (ca. 12,000 BP) and with an exponential drop associated to the newly suggested geological epoch of the Anthropocene (ca. from 0 BP = 1950 AD, Steffen et al. 2016).

Considering that the variation in $\delta^{13}\text{C}_{\text{plant}}$ values with time induce the change in the isotopic signature of the soil carbon input, we were able to derive its impact on

Fig. 2 **a.** Overall depth distribution of $\delta^{13}\text{C}_{\text{SOM}}$ values and **b.** Mean calendar age calculated with Eq. 5 in the 45 soil profiles



SOM $\delta^{13}\text{C}$ values. Simulated data, $\delta^{13}\text{C}_{\text{sim}}$ values, mimicked the measured data, $\delta^{13}\text{C}_{\text{SOM}}$ values in Fig. 4b and showed a relation with a slope close to 1 (Fig. 5) although $\delta^{13}\text{C}_{\text{SOM}}$ values are enriched compared to $\delta^{13}\text{C}_{\text{sim}}$ values for the old layers. The $\delta^{13}\text{C}_{\text{SOM}}$ and $\delta^{13}\text{C}_{\text{sim}}$ values in Fig. 5 were obtained independently: $\delta^{13}\text{C}_{\text{sim}}$ values were deduced from the ecophysiological literature (Eq. 6), whereas $\delta^{13}\text{C}_{\text{SOM}}$ values were

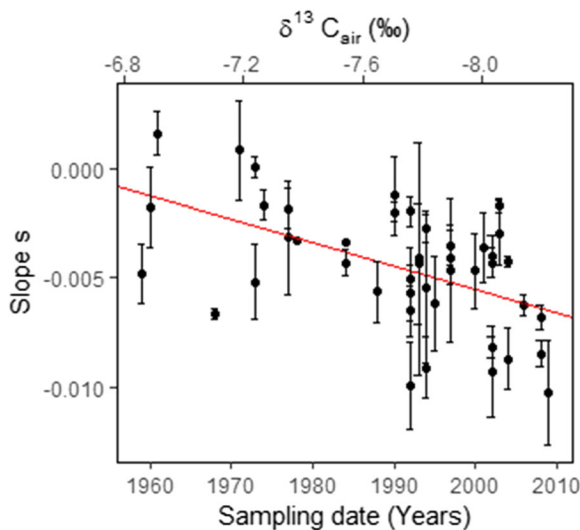


Fig. 3 Relation between the slope s and the sampling date of each profile, or the mean isotopic composition of the atmospheric ($\delta^{13}\text{C}_{\text{air}}$ values) at the corresponding year; s is the slope of the linear regression of $\delta^{13}\text{C}_{\text{SOM}}$ values as a function of $\Delta^{14}\text{C}_{\text{SOM}}$ values of an individual profile. The red line and the equation on the graph correspond to the regression of the slopes s vs the sampling dates. Error bars represent one standard error of the estimated slope s in each profile. See Table 1 for definitions of variables and abbreviations

obtained from the soil database (Supplementary material). To express $\delta^{13}\text{C}_{\text{SOM}}$ values variations with time, and thus to derive age in years from $\Delta^{14}\text{C}_{\text{SOM}}$ values, we chose an exponential hypothesis to express the fact that mean age of SOM (Eq. 5) is the mixture of young and older compounds in each sample. This is an oversimplification of the soil carbon demography, but is in accordance with the observed smoothing of the bomb- ^{14}C peak of the 1960s. The latter is delayed and diluted in SOM as observed by O'Brien and Stout (1978) and Trumbore (2009). The exponential hypothesis has no final impact on the general relation between $\delta^{13}\text{C}_{\text{SOM}}$ and $\delta^{13}\text{C}_{\text{sim}}$ values, since $\delta^{13}\text{C}_{\text{sim}}$ values and calendar age from $\Delta^{14}\text{C}$ values were calculated using the same distribution of ages. Consequently, the relation revealed in Fig. 5 between $\delta^{13}\text{C}_{\text{SOM}}$ and $\delta^{13}\text{C}_{\text{sim}}$ values is real and not an artifact of data handling: 40% of soil organic matter isotopic signal with depth is explained by the variations of isotopic composition of vegetation with time by only considering average changes in atmospheric CO_2 . The relation of $\delta^{13}\text{C}_{\text{SOM}}$ values with elevation also suggests the impact of pCO_2 on $\delta^{13}\text{C}_{\text{plant}}$ values but was not taken into account in our linear models that only consider mean global reconstructed pCO_2 .

In addition to changes in pCO_2 , and subsequent $\delta^{13}\text{C}_{\text{plant}}$ values, $\delta^{13}\text{C}$ values enrichment in SOM might be caused by post-photosynthesis fractionation observed in different plant organs (Badeck et al. 2005; Brüggemann et al. 2011). In fact, C_3 plants roots are ^{13}C -enriched by 1.2 ± 0.6 ‰ compared to the shoots (Klumpp et al. 2005; Badeck et al. 2005; Werth and Kuzyakov 2006). Moreover, the proportion of root-derived C inputs is expected to be higher at depth

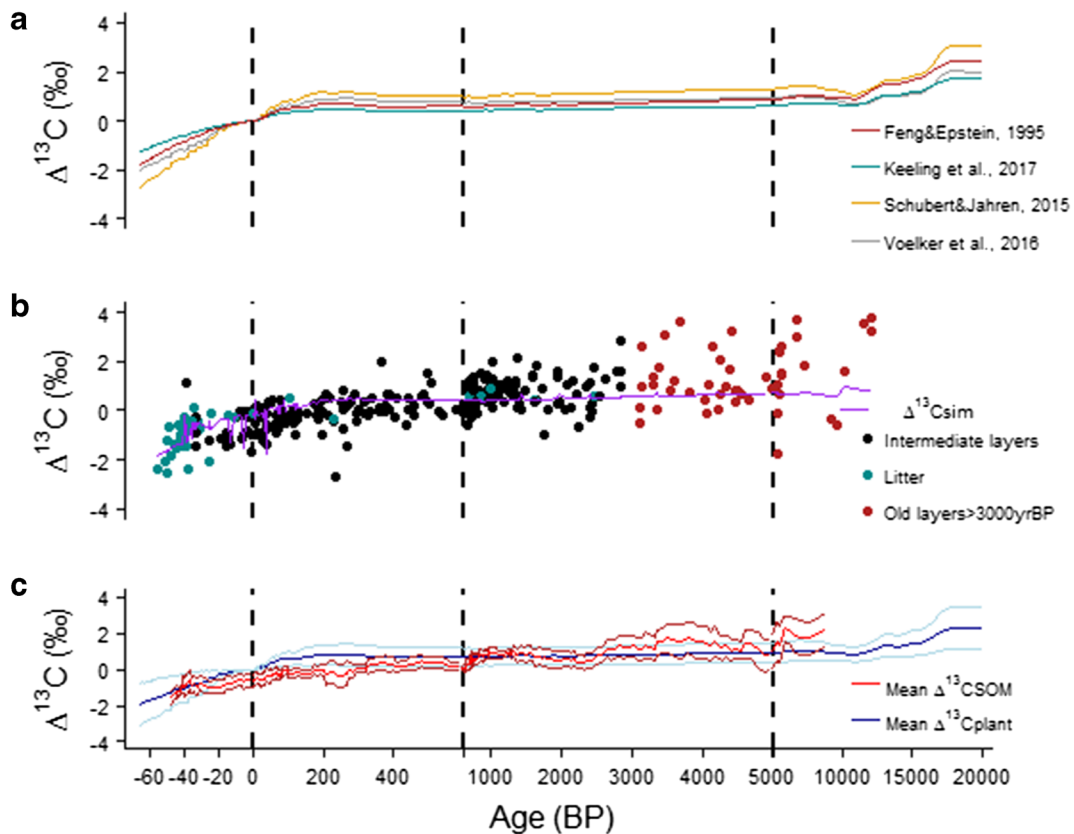


Fig. 4 a. Reconstruction of $\Delta^{13}\text{C}_{\text{plant}}$ values from 20,000 BP to today from 4 different studies. b. $\delta^{13}\text{C}_{\text{SOM}}$ values as a function of the mean calendar age of each SOM sample and $\delta^{13}\text{C}_{\text{sim}}$ calculated with Eq. 6. The age was inferred from $\Delta^{14}\text{C}_{\text{SOM}}$ and sampling date, using Eq. 5. c. Mean values of $\Delta^{13}\text{C}_{\text{plant}}$ and $\Delta^{13}\text{C}_{\text{SOM}}$ (moving average of 10 points). The light-blue lines represent two

standard errors of the estimated mean value $\Delta^{13}\text{C}_{\text{plant}}$ from the four scenarios; it does not take into account the error of each individual scenario. The light-red lines represent the confidence interval of the mean value $\Delta^{13}\text{C}_{\text{SOM}}$ (95%). Note that the x axis is divided into 4 scales. See Table 1 for definitions of variables and abbreviations

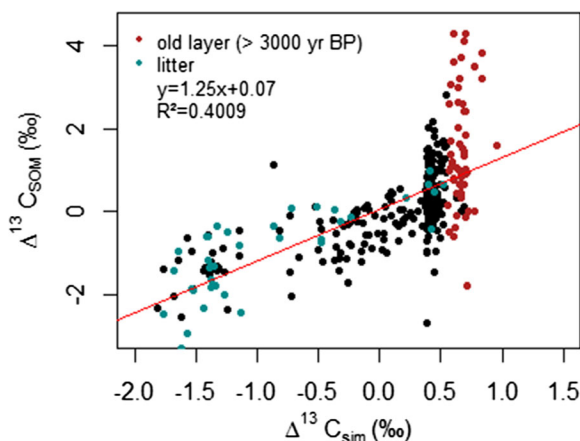


Fig. 5 Observed $\Delta^{13}\text{C}_{\text{SOM}}$ versus $\Delta^{13}\text{C}_{\text{sim}}$ values, predicted from the sole hypothesis of a past change in $\delta^{13}\text{C}_{\text{plant}}$ values. Highlighting of layers older than 3000 BP in red and litter in blue. The red line is the linear regression. See Table 1 for definitions of variables and abbreviations

(e.g., from <40% of inputs at 0 cm to more than 80% at 100 cm) depending on the contribution of dissolved organic carbon in deep horizons (Balesdent et al. 2011). The proportion of root-derived C could even be higher in boreal environments where 50 to 70% of organic matter are derived from roots and root-associated microorganisms, especially ectomycorrhizal fungi (Clemmensen et al. 2013). The ^{13}C root enrichment was not included in our simulation and could be the reason for the deviation from unity in the relation with $\delta^{13}\text{C}_{\text{SOM}}$ values (Figs. 4b and 5). Indeed, using this assumption, a ^{13}C root enrichment of 1.2 ± 0.6 ‰ (Werth and Kuzyakov 2006) would contribute at least to an additional SOM enrichment, accounting for 0.5 ± 0.2 ‰ in the 0 and 1 m soil depth. Notably, this value corresponds to the observed difference between the overall depth gradient of $\Delta^{13}\text{C}_{\text{SOM}}$ and $\Delta^{13}\text{C}_{\text{sim}}$ values (Figs. 4 and 5). Therefore, we suggest that more than the

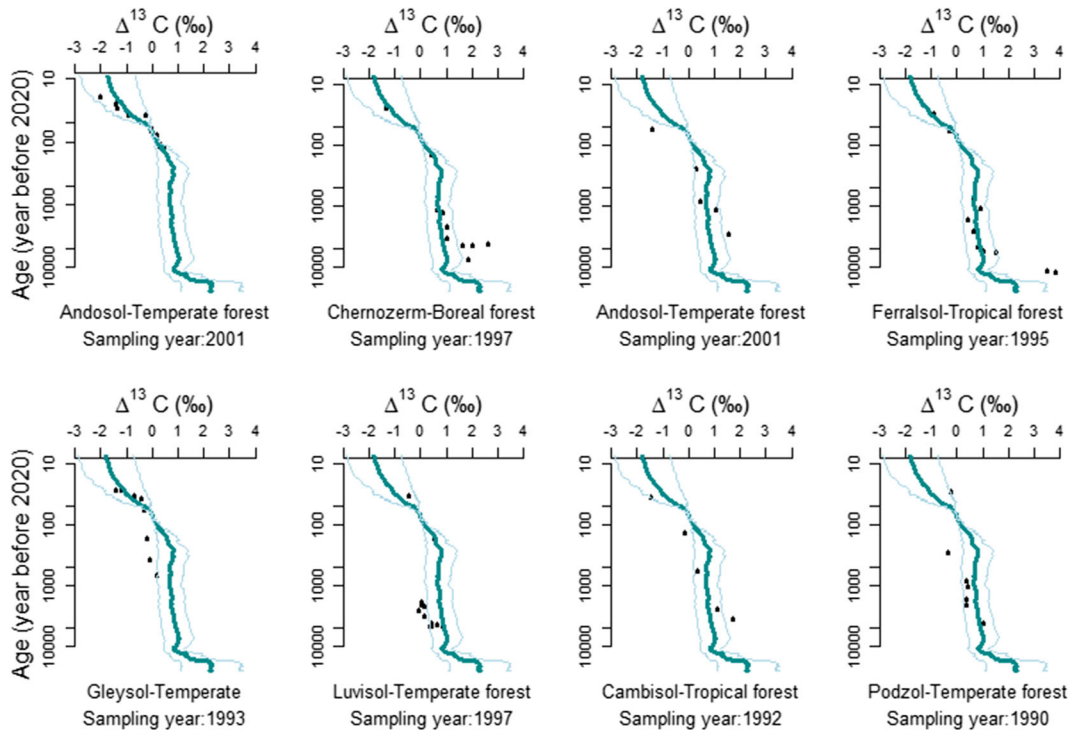


Fig. 6 $\Delta^{13}\text{C}_{\text{SOM}}$ values of 8 selected soil profiles (black dot) representing the major soil types, climates and land cover of the database compared to the global trend $\Delta^{13}\text{C}_{\text{plant}}$ values (in blue) in function of the age (year before 2020). The Y-axis is the mean

calendar age of SOM inferred from $\Delta^{14}\text{C}_{\text{SOM}}$ values and sampling date from 2020. The light-blue lines represent two standard errors of the estimated mean value $\Delta^{13}\text{C}_{\text{plant}}$. See Table 1 for definitions of variables and abbreviations

half of the ^{13}C -enrichment in SOM is directly derived by $\delta^{13}\text{C}_{\text{plant}}$ values, including root derived carbon.

Variations in $\delta^{13}\text{C}$ values due to plant and soil diversity

Our results have shown that changes over time of $\delta^{13}\text{C}_{\text{plant}}$ values explain at least 40% of SOM $\delta^{13}\text{C}$ values variations (Fig. 5). However, the reason of the uncertainty around the trend (Figs. 4 and 5) was not explained by our model. First of all, we have chosen to use a global $\delta^{13}\text{C}_{\text{plant}}$ value over time based on the average of Eqs. 1, 2, 3 and 4 excluding the effect of local climate or different types of vegetation. Therefore, the variance around the change in $\delta^{13}\text{C}$ values with time might be due to the spatial variation associated with differences in plant species and the temporal variation of vegetation element (e.g. shrubs, grass, forests), that may have occurred on a given site. Indeed, photosynthetic $\delta^{13}\text{C}$ values discrimination in the plant is sensitive to various environmental conditions such as light and water (Farquhar et al. 1989) and to vegetation type (Brugnoli and Farquhar 2000), on the plant genotype

(Roussel et al. 2009) and nutritional status. Balesdent et al. (1993) have for instance reported that the variance of $\delta^{13}\text{C}$ values of the different plant species in a single forest was almost as large as the variance of the vegetation $\delta^{13}\text{C}$ values in the world. Plant $\delta^{13}\text{C}$ values were mainly determined by local pedoclimate; i.e. soil microclimates controlled by local temperature, water content and aeration of the soil. Since plant species react differently to environmental changes with different fractionation factors (Ehleringer and Cerling 1995; Voelker et al. 2016), the $\delta^{13}\text{C}$ values of vegetation as a function of age record the local changes, also observed in SOM.

The relation of climatic variables and ecosystem type with s values (Fig. 3) were not detectable in our dataset but could be partly responsible for the variance around the trend.

Different soil types and pedogenesis also had an impact on the variation in $\delta^{13}\text{C}$ values. Beyond the date of sampling, organic matter represented a relative ^{13}C depletion of 2‰ on average compared to the $\delta^{13}\text{C}_{\text{plant}}$ values in soils, in which the pedogenesis is controlled by percolating processes or low clay content (Podzol,

Cambisol) in intermediate age (between 100 and 1000 BP). For instance, $\delta^{13}\text{C}_{\text{SOM}}$ values of the Podzols in the database have decreased on average by only 0.98‰ between 2500 BP and –40 BP compared to the 1.82‰ on average for the other soils. Therefore, soil processes such as interaction with the inorganic phase and/or organic carbon dissolution (Kaiser et al. 2001) could create variance in the generally predicted $\delta^{13}\text{C}$ values profile. Wynn et al. (2005) found that fine-textured soils lead to the selective accumulation of ^{13}C -enriched components of SOM (carbohydrates, bases, amino acids) and also protect microbial compounds. The texture of the soil selected in this database was not always reported impeding to confirm this statement. However, soil texture is likely one of the cause of variations and differences in ^{13}C enrichment among soil profiles.

$\delta^{13}\text{C}_{\text{SOM}}$ values enrichment due to microbial processes

From our results, $\delta^{13}\text{C}_{\text{plant}}$ values cannot explain the whole ^{13}C gradient in SOM (Fig. 5). Previous explanations of the $\delta^{13}\text{C}$ values enrichment with depth during soil processes were kinetic discrimination during respiration, preferential consumption of compounds and contribution of sorption processes.

The first hypothesis is the preference of ^{12}C for respiration by micro-organisms (Agren et al. 1996; Ekblad et al. 2002). Since organic matter is mainly composed of microbe-derived products more than from plant-derived molecules (Bol et al. 2009), this discrimination during respiration should affect $\delta^{13}\text{C}_{\text{SOM}}$ values when age of SOM increases. Laboratory experiments on respired CO_2 from soils have resulted in contrasted fractionation. Werth and Kuzyakov (2010) by synthesizing several results have found a $\delta^{13}\text{C}$ values difference between respired CO_2 and soil microbial biomass between +4.6‰ and –3.2‰. This large variation could be due to the different methods used for CO_2 sampling or to different carbon sources used by micro-organisms (Boström et al. 2007) and did not support the hypothesis. The nature of substrate may affect more the isotopic composition of CO_2 than the fractionation process itself during respiration (Fernandez and Cadisch 2003). Since micro-organisms preferentially mineralize carbon that is more accessible which corresponds to younger carbon in accordance with the continuous litter quality theory (Agren et al. 1996; Lehmann and Kleber 2015); we suggest that a part of the respired CO_2 is ^{13}C -depleted compared to SOM because fresh carbon

(young carbon) is ^{13}C -depleted. Therefore, the isotope discrimination associated to the respiration would have a lower contribution to the depth gradients, in accordance with the conclusion of Boström et al. (2007) or Breecker et al. (2015) and in contrast with the hypothesis of Agren et al. (1996).

The microbial biomass is also ^{13}C -enriched by 1.2 ± 2.6 ‰ compared to SOM (Werth and Kuzyakov 2010). This suggests a preferential utilization of ^{13}C -enriched compounds by micro-organisms because hardly decomposable compounds are generally ^{13}C -depleted such as lignin and lipids compared to proteins or starch (Bowling et al. 2008). However, lignin is degraded quickly in soils (Kögel-Knabner 2000). Microbial biomass is able to decompose any kind of organic compounds which are accessible but the protection of some organic compounds by organo-mineral interaction could induce preferential use during biodegradation (Lützow et al. 2006). In addition, microorganisms are mainly composed of root-derived carbon in soils (Kramer et al. 2010; Schmidt et al. 2011; Clemmensen et al. 2013), generally enriched compared to the aboveground vegetation leading to an enrichment with depth of carbon biomass. Hence, true mass-dependent isotope fractionation may be compensated by isotope effects in opposite direction, such as preferential use or absorption of compounds with varying $\delta^{13}\text{C}$ values during stabilization or degradation. ^{13}C -enrichment in soil during biodegradation processes cannot be systematic. However, $\delta^{13}\text{C}_{\text{SOM}}$ values are generally enriched relative to $\delta^{13}\text{C}_{\text{sim}}$ values for the old layers (> 3000 yr BP, Figs. 4 and 5); suggesting a ^{13}C -enrichment of SOM relative to the global trend $\delta^{13}\text{C}_{\text{plant}}$ values due to microbial processes during the time course of decomposition. But in addition to the discrimination associated with biodegradation and to the post-photosynthesis fractionation, we propose another hypothesis for the very high values of $\Delta\delta^{13}\text{C}_{\text{SOM}}$ in Figs. 4 and 5, i.e., the contribution of old organic matter from Pleistocene vegetation which is ^{13}C -enriched (Fig. 4). As mentioned, a number of processes might have led to accumulation of ^{13}C -enriched past vegetation and subsequent stabilization of older carbon at depth; such as successive degradation stages of SOM (Lehmann and Kleber 2015), the mineral protection of organic compounds (Basile-Doelsch et al. 2015) and the lack of energy needed for micro-organisms to decompose organic matter in deep layers (Fontaine et al. 2007). Another possible source of carbon in subsoils is dissolved organic carbon coming from

desorption and dissolution of organic compounds during microbial processes (Kaiser et al. 2001) and becoming older with deep transport. Further research is needed regarding the quantification of ^{13}C enrichment in SOM in subsoils due to microbial processes.

Conclusion

^{13}C enrichment of soil organic matter with depth is commonly recorded in soil profiles worldwide. Disentangling its origin before using this variable as conservative to yield information of the composition of soil organic matter mixture or any soil process is a prerequisite aiming at defining organic matter dynamics. Here, atmospheric and paleoclimatic data of CO_2 , four physiological models to reconstruct past $\delta^{13}\text{C}$ values of vegetation and soil radiocarbon data revealed that the variation of past vegetation $\delta^{13}\text{C}$ values is an important reason of the average $\delta^{13}\text{C}$ values enrichment in soil with depth. Around the global trend, three other mechanisms may affect $\delta^{13}\text{C}$ values of SOM: i) The increasing contribution of root-derived carbon with increasing depth results in a general ^{13}C enrichment in soil carbon with increasing depth - ii) Soil processes which may lead to weaker or stronger ^{13}C gradients for example by accumulation of ^{13}C -depleted components in low-clay soils such as podzols and cambisols- iii) The discrimination associated with microbial processes which may lead to the accumulation of ^{13}C -enriched compounds during the decomposition of SOM.

We suggest that above and below ground vegetation $\delta^{13}\text{C}$ values, all together, could even be the only reason of the ^{13}C variations in SOM with minor alterations due to soil processes.

Finally, considering that the stable isotopic composition of soil carbon is related to the absolute age of organic matter, the large change in C_3 plant isotopic composition associated with the Anthropocene may provide an indication of the age of soil carbon in topsoils in a “ ^{13}C dating” approach. The change in pCO_2 during the Anthropocene is sufficient to estimate the age within the last 100 years. Since the mean residence time of SOM in topsoil lies between decades and centuries, dating SOM in that range is of particular interest. Moreover, “ ^{13}C -dating” in combination with radiocarbon dating is accordingly a potential tool to separate the $\Delta^{14}\text{C}$ values before and after the bomb signal. This method may be complementary to radiocarbon dating.

Acknowledgements This work contributes to the INSU-EC2CO Dyvertis, and the ANR-Dedycas (ANR-14-CE01-0004) projects. Andra, Research and Development Division, and EDF R&D are gratefully acknowledged for having funded Alexia Paul. We are also very grateful to the anonymous reviewers for the comments and the improvements they have made on the manuscript.

References

- Agren GI, Bosatta E, Balesdent J (1996) Isotope discrimination during decomposition of organic matter: a theoretical analysis. *Soil Sci Soc Am J* 60:1121–1126
- Badeck F-W, Tcherkez G, Nogués S, Piel C, Ghashghaie J (2005) Post-photosynthetic fractionation of stable carbon isotopes between plant organs—a widespread phenomenon. *Rapid Commun Mass Spectrom* 19:1381–1391. <https://doi.org/10.1002/rcm.1912>
- Balesdent J (1987) The turnover of soil organic fractions estimated by radiocarbon dating. *Sci Total Environ* 62:405–408. [https://doi.org/10.1016/0048-9697\(87\)90528-6](https://doi.org/10.1016/0048-9697(87)90528-6)
- Balesdent J, Girardin C, Mariotti A (1993) Site-Related Delta- ^{13}C of tree leaves and soil organic-matter in a temperate Forest. *Ecology* 74:1713–1721. <https://doi.org/10.2307/1939930>
- Balesdent J, Derrien D, Fontaine S et al (2011) Contribution de la rhizodéposition aux matières organiques du sol, quelques implications pour la modélisation de la dynamique du carbone. *Etude Gest Sols* 18:201–216
- Balesdent J, Basile-Doelsch I, Chadoeuf J, Cornu S, Derrien D, Fekiacova Z, Hatté C (2018) Atmosphere-soil carbon transfer as a function of soil depth. *Nature* 559:599–602. <https://doi.org/10.1038/s41586-018-0328-3>
- Basile-Doelsch I, Balesdent J, Rose J (2015) Are interactions between organic compounds and Nanoscale weathering minerals the key drivers of carbon storage in soils? *Environ Sci Technol* 49:3997–3998. <https://doi.org/10.1021/acs.est.5b00650>
- Bol R, Poirier N, Balesdent J, Gleixner G (2009) Molecular turnover time of soil organic matter in particle-size fractions of an arable soil. *Rapid Commun Mass Spectrom* 23:2551–2558
- Boström B, Comstedt D, Ekblad A (2007) Isotope fractionation and ^{13}C enrichment in soil profiles during the decomposition of soil organic matter. *Oecologia* 153:89–98. <https://doi.org/10.1007/s00442-007-0700-8>
- Bowling DR, Pataki DE, Randerson JT (2008) Carbon isotopes in terrestrial ecosystem pools and CO_2 fluxes. *New Phytol* 178: 24–40. <https://doi.org/10.1111/j.1469-8137.2007.02342.x>
- Breecker DO, Bergel S, Nadel M, Tremblay MM, Osuna-Orozco R, Larson TE, Sharp ZD (2015) Minor stable carbon isotope fractionation between respired carbon dioxide and bulk soil organic matter during laboratory incubation of topsoil. *Biogeochemistry* 123:83–98. <https://doi.org/10.1007/s10533-014-0054-3>
- Brüggemann N, Gessler A, Kayler Z et al (2011) Carbon allocation and carbon isotope fluxes in the plant-soil-atmosphere

- continuum: a review. *Biogeosciences* 8:3457–3489. <https://doi.org/10.5194/bg-8-3457-2011>
- Brugnoli E, Farquhar GD (2000) Photosynthetic fractionation of carbon isotopes. In: Leegood RC, Sharkey TD, von Caemmerer S (eds) *Photosynthesis*. Springer Netherlands, Dordrecht pp 399–434
- Brunn M, Condron L, Wells A, Spielvogel S, Oelmann Y (2016) Vertical distribution of carbon and nitrogen stable isotope ratios in topsoils across a temperate rainforest dune chronosequence in New Zealand. *Biogeochemistry* 129:37–51. <https://doi.org/10.1007/s10533-016-0218-4>
- Brunn M, Brodbeck S, Oelmann Y (2017) Three decades following afforestation are sufficient to yield $\delta^{13}\text{C}$ depth profiles. *J Plant Nutr Soil Sci* 180:643–647. <https://doi.org/10.1002/jpln.201700015>
- Campbell CA, Paul EA, Rennie DA, McCallum KJ (1967) Applicability of the carbon-dating method of analysis to soil humus studies. *Soil Sci* 104:217
- Clemmensen KE, Bahr A, Ovaskainen O et al (2013) Roots and associated Fungi drive long-term carbon sequestration in boreal Forest. *Science* 339:1615–1618. <https://doi.org/10.1126/science.1231923>
- Van de Water PK, Leavitt SW, Betancourt JL (1994) Trends in Stomatal density and $^{13}\text{C}/^{12}\text{C}$ ratios of *Pinus flexilis* needles during last glacial-interglacial cycle. *Science* 264:239–243. <https://doi.org/10.1126/science.264.5156.239>
- Ehleringer JR, Cerling TE (1995) Atmospheric CO_2 and the ratio of intercellular to ambient CO_2 concentrations in plants. *Tree Physiol* 15:105–111. <https://doi.org/10.1093/treephys/15.2.105>
- Ekblad A, Nyberg G, Höglberg P (2002) ^{13}C -discrimination during microbial respiration of added C_3 -, C_4 - and ^{13}C -labelled sugars to a C_3 -forest soil. *Oecologia* 131:245–249. <https://doi.org/10.1007/s00442-002-0869-9>
- Elzein A, Balesdent J (1995) A mechanistic simulation of the vertical distribution of carbon concentrations and residence times in soils. *Soil Sci Soc Am* 59:1328–1335
- Farquhar GD, Ehleringer JR, Hubick KT (1989) Carbon isotope discrimination and photosynthesis. *Annu Rev Plant Physiol Plant Mol Biol* 40:503–537. <https://doi.org/10.1146/annurev.pp.40.060189.002443>
- Feng X, Epstein S (1995) Carbon isotopes of trees from arid environments and implications for reconstructing atmospheric CO_2 concentration. *Geochim Cosmochim Acta* 59:2599–2608. [https://doi.org/10.1016/0016-7037\(95\)00152-2](https://doi.org/10.1016/0016-7037(95)00152-2)
- Fernandez I, Cadisch G (2003) Discrimination against ^{13}C during degradation of simple and complex substrates by two white rot fungi. *Rapid Commun Mass Spectrom* 17:2614–2620. <https://doi.org/10.1002/rcm.1234>
- Fontaine S, Barot S, Barré P, Bdioui N, Mary B, Rumpel C (2007) Stability of organic carbon in deep soil layers controlled by fresh carbon supply. *Nature* 450:277–280. <https://doi.org/10.1038/nature06275>
- Francey RJ, Allison CE, Etheridge DM et al (1999) A 1000-year high precision record of $\delta^{13}\text{C}$ in atmospheric CO_2 . *Tellus B* 51. <https://doi.org/10.3402/tellusb.v51i2.16269>
- Gaudinski JB, Trumbore SE, Davidson EA, Zheng S (2000) Soil carbon cycling in a temperate forest: radiocarbon-based estimates of residence times, sequestration rates and partitioning of fluxes. *Biogeochemistry* 51:33–69. <https://doi.org/10.1023/A:1006301010014>
- Gessler A, Keitel C, Kodama N, et al (2007) Delta C-13 of organic matter transported from the leaves to the roots in *Eucalyptus delegatensis*: short-term variations and relation to respired CO_2
- He Y, Trumbore SE, Torn MS, Harden JW, Vaughn LJ, Allison SD, Randerson JT (2016) Radiocarbon constraints imply reduced carbon uptake by soils during the 21st century. *Science* 353:1419–1424. <https://doi.org/10.1126/science.aad4273>
- Hua Q, Barbetti M, Rakowski A (2013) Atmospheric radiocarbon for the period 1950–2010. *Radiocarbon* 55:2059–2072. https://doi.org/10.2458/azu_js_rc.v55i2.16177
- IUSS Working Group WRB (2014) World reference base for soil resources 2014: international soil classification system for naming soils and creating legends for soil maps. FAO, Rome
- Jobbagy EG, Jackson RB (2000) The vertical distribution of soil organic carbon and its relation to climate and vegetation. *Ecol Appl* 10:423. <https://doi.org/10.2307/2641104>
- Kaiser K, Guggenberger G, Zech W (2001) Isotopic fractionation of dissolved organic carbon in shallow forest soils as affected by sorption. *Eur J Soil Sci* 52:585–597. <https://doi.org/10.1046/j.1365-2389.2001.00407.x>
- Keeling CD, Mook WG, Tans PP (1979) Recent trends in the $^{13}\text{C}/^{12}\text{C}$ ratio of atmospheric carbon dioxide. *Nature* 277:121–123. <https://doi.org/10.1038/277121a0>
- Keeling CD, Whorf TP, Wahlen M, van der Plicht J (1995) Interannual extremes in the rate of rise of atmospheric carbon dioxide since 1980. *Nature* 375:666–670. <https://doi.org/10.1038/375666a0>
- Keeling RF, Graven HD, Welp LR et al (2017) Atmospheric evidence for a global secular increase in carbon isotopic discrimination of land photosynthesis. *Proc Natl Acad Sci* 114:10361–10366
- Klump K, Schäufele R, Lötscher M et al (2005) C-isotope composition of CO_2 respired by shoots and roots: fractionation during dark respiration? *Plant Cell Environ* 28:241–250. <https://doi.org/10.1111/j.1365-3040.2004.01268.x>
- Kögel-Knabner I (2000) Analytical approaches for characterizing soil organic matter. *Org Geochem* 31:609–625. [https://doi.org/10.1016/S0146-6380\(00\)00042-5](https://doi.org/10.1016/S0146-6380(00)00042-5)
- Kohn MJ (2016) Carbon isotope discrimination in C_3 land plants is independent of natural variations in pCO_2 . *Geochemical Perspectives Letters*:35–43
- Kramer C, Trumbore S, Fröberg M et al (2010) Recent (<4 year old) leaf litter is not a major source of microbial carbon in a temperate forest mineral soil. *Soil Biol Biochem* 42:1028–1037. <https://doi.org/10.1016/j.soilbio.2010.02.021>
- Krishnamurthy R, Epstein S (1990) Glacial-interglacial excursion in the concentration of atmospheric CO_2 - effect in the C-13/C-12 ratio in wood cellulose. *Tellus Ser B-Chem Phys Meteorol* 42:423–434. <https://doi.org/10.1034/j.1600-0889.1990.t01-5-00003.x>
- Lehmann J, Kleber M (2015) The contentious nature of soil organic matter. *Nature* 528:60–68. <https://doi.org/10.1038/nature16069>
- Lützwow MV, Kögel-Knabner I, Ekschmitt K et al (2006) Stabilization of organic matter in temperate soils: mechanisms and their relevance under different soil conditions – a review. *Eur J Soil Sci* 57:426–445. <https://doi.org/10.1111/j.1365-2389.2006.00809.x>

- Mathieu JA, Hatté C, Balesdent J, Parent É (2015) Deep soil carbon dynamics are driven more by soil type than by climate: a worldwide meta-analysis of radiocarbon profiles. *Glob Chang Biol* 21:4278–4292. <https://doi.org/10.1111/gcb.13012>
- New M, Lister D, Hulme M, Makin I (2002) A high-resolution data set of surface climate over global land areas. *Clim Res* 21:1–15
- O'Brien BJ, Stout JD (1978) Movement and turnover of soil organic matter as indicated by carbon isotope measurements. *Soil Biol Biochem* 10:309–317. [https://doi.org/10.1016/0038-0717\(78\)90028-7](https://doi.org/10.1016/0038-0717(78)90028-7)
- Pasquier-Cardin A, Allard P, Ferreira T et al (1999) Magma-derived CO₂ emissions recorded in ¹⁴C and ¹³C content of plants growing in Furnas caldera, Azores. *J Volcanol Geotherm Res* 92:195–207. [https://doi.org/10.1016/S0377-0273\(99\)00076-1](https://doi.org/10.1016/S0377-0273(99)00076-1)
- Poage MA, Feng X (2004) A theoretical analysis of steady state δ¹³C profiles of soil organic matter: CARBON ISOTOPE PROFILES IN SOILS. *Glob Biogeochem Cycles* 18. <https://doi.org/10.1029/2003GB002195>
- Rafter TA, Stout JD (1970) Radiocarbon measurements as an index of the rate of turnover of organic matter in forest and grassland ecosystems in New Zealand. In: *Radiocarbon Variations and Absolute Chronology*. I.U. Oisson, Stockholm, pp 401–418
- Reimer PJ, Bard E, Bayliss A, et al (2009) IntCal09 and Marine09 radiocarbon age calibration curves, 0–50,000 years cal BP
- Roussel M, Dreyer E, Montpied P, le-Provost G, Guehl JM, Brendel O (2009) The diversity of ¹³C isotope discrimination in a *Quercus robur* full-sib family is associated with differences in intrinsic water use efficiency, transpiration efficiency, and stomatal conductance. *J Exp Bot* 60:2419–2431. <https://doi.org/10.1093/jxb/erp100>
- Šantrůčková H, Kotas P, Bárta J et al (2018) Significance of dark CO₂ fixation in arctic soils. *Soil Biol Biochem* 119:11–21. <https://doi.org/10.1016/j.soilbio.2017.12.021>
- Schmidt MWI, Torn MS, Abiven S et al (2011) Persistence of soil organic matter as an ecosystem property. *Nature* 478:49–56. <https://doi.org/10.1038/nature10386>
- Schmitt J, Schneider R, Elsig J et al (2012) Carbon isotope constraints on the Deglacial CO₂ rise from ice cores. *Science* 336:711–714. <https://doi.org/10.1126/science.1217161>
- Schubert BA, Jahren AH (2015) Global increase in plant carbon isotope fractionation following the last glacial maximum caused by increase in atmospheric pCO₂. *Geology* 43:435–438. <https://doi.org/10.1130/G36467.1>
- Steffen W, Leinfelder R, Zalasiewicz J, Waters CN, Williams M, Summerhayes C, Barnosky AD, Cearreta A, Crutzen P, Edgeworth M, Ellis EC, Fairchild IJ, Galuszka A, Grinevald J, Haywood A, Ivar do Sul J, Jeandel C, McNeill JR, Odada E, Oreskes N, Revkin A, Richter DdeB, Syvitski J, Vidas D, Wagemann M, Wing SL, Wolfe AP, Schellnhuber HJ (2016) Stratigraphic and Earth System approaches to defining the Anthropocene. *Earth's Future* 4(8):324–345
- Trabucco A, Zomer R (2009) Global aridity index (global-aridity) and global potential Evapo-transpiration (Global-PET) geospatial database. CGIAR, consortium for spatial information
- Trumbore S (2009) Radiocarbon and soil carbon dynamics. *Annu Rev Earth Planet Sci* 37:47–66. <https://doi.org/10.1146/annurev.earth.36.031207.124300>
- US Department of Commerce (2017) N ESRL Global Monitoring Division - Global Greenhouse Gas Reference Network. <https://www.esrl.noaa.gov/gmd/ccgg/trends/data.html>. Accessed 18 Apr 2017
- Voelker SL, Brooks JR, Meinzer FC et al (2016) A dynamic leaf gas-exchange strategy is conserved in woody plants under changing ambient CO₂: evidence from carbon isotope discrimination in paleo and CO₂ enrichment studies. *Glob Chang Biol* 22:889–902. <https://doi.org/10.1111/gcb.13102>
- Wang C, Houlton BZ, Liu D et al (2018) Stable isotopic constraints on global soil organic carbon turnover. *Biogeosciences* 15:987–995. <https://doi.org/10.5194/bg-15-987-2018>
- Werth M, Kuzyakov Y (2006) Assimilate partitioning affects ¹³C fractionation of recently assimilated carbon in maize. *Plant Soil* 284:319–333. <https://doi.org/10.1007/s11104-006-0054-8>
- Werth M, Kuzyakov Y (2010) ¹³C fractionation at the root-microorganisms-soil interface: a review and outlook for partitioning studies. *Soil Biol Biochem* 42:1372–1384
- Wynn JG, Bird MI, Wong VNL (2005) Rayleigh distillation and the depth profile of ¹³C/¹²C ratios of soil organic carbon from soils of disparate texture in Iron range National Park, far North Queensland, Australia. *Geochim Cosmochim Acta* 69:1961–1973. <https://doi.org/10.1016/j.gca.2004.09.003>

Publisher's note Springer Nature remains neutral with regard to jurisdictional claims in published maps and institutional affiliations.